EVALUATION OF CGCM AND SIMULATION OF REGIONAL CLIMATE CHANGE IN EAST ASIA*

Li Xiaodong (李晓东),

Department of Geophysics, Peking University, Beijing 100871

Zhao Zongci (赵宗慈),

Chinese Academy of Meteorological Sciences, Beijing 100081

Wang Shaowu (王绍武)

Department of Geophysics, Peking University, Beijing 100871

and *Ding Yihui* (丁一汇)

Chinese Academy of Meteorological Sciences, Beijing 100081

Received January 9, 1995; revised March 14, 1995

ABSTRACT

In this paper, experiment results about East Asia climate from five CGCMs are described. The ability of the models to simulate present climate and the simulated response to increased carbon dioxide are both covered. The results indicate that all models show substantial changes in climate when carbon dioxide concentrations are doubled. In particular, the strong surface warming at high latitudes in winter and the significant increase of summer precipitation in the monsoon area are produced by all models. Regional evaluation results show that these five CGCMs are particularly good in simulating spatial distribution of present climate. The main characteristics of the seasonal mean H500, SAT, MSLP field can be simulated by most CGCMs. But there are significant systematic errors in SAT, MSLP, H500 fields in most models. On the whole, DKRZ OPYC is the best in simulating the present climate in East Asia.

Key words: evaluation, coupled atmosphere and ocean genéral circulation model (CGCM), transient simulation, climate change

I. INTRODUCTION

Since the Intergovernmental Panel on Climate Change (IPCC) introduced a project, called "Evaluation of regional climate simulations" (IPCC WGI 1994a), there have been significant advances in modeling the present climate and in simulating the climate change induced by increasing CO_2. Previous studies were often concerned with global or large scale — such as continental scale. However, more researches are presently carrying out regional studies — corresponding to smaller scale (subcontinental scale). There are several areas chosen by IPCC

* The work was supported by the National Science and Technical Committee in China (85-913-02-05), Climate Prediction Program and the National Postdocter Fund.

WGI as the fundamental regions for the subcontinent scale study. The East Asia area is one of them. In the late 1993, IPCC collected a group of coupled atmosphere and ocean general circulation model (CGCM) performance results to undertake this study. These CGCM experiments are: DKRZ OPYC (Max-Plank Institute, FGR), DKRZ LSG (Max-Plank Institute, FGR), NCAR (the National Center for Atmospheric Research, USA), GFDL (Geophysical Fluid Dynamics Laboratory, USA), and HADL (Hadley Center, UK), as shown in Table 1. In several previous meetings (IPCC WGI 1994a; 1994b), there have been some regional study papers reported.

Table 1. Summary of Available CGCM Experiments

CGCMs	DKRZ OPYC	DKRZ LSG	NCAR	GFDL	HADL
Reference	Cubash et al. 1992, 1993	Cubash et al. 1992, 1993	Washington and Meehl 1989—1993	Manabe et al. 1989—1993	Mitchell et al. 1992—1993
Resolution (AGCM)	T21 L19	T21 L19	R15 L9	R15 L9	2.5°×3.75°
Resolution (OGCM)	5.6°×5.6° L17	4°×4° L11	5°×5° L4	4.5°×3.75° L12	2.5°×3.75° L17
CO_2 increasing	IPCC 1990 A	IPCC 1990 A	1% /a	1% /a	1% /a
CO_2 concentr. (contr. run)	390 ppmv	390 ppmv	330 ppmv	300 ppmv	323 ppmv
Years (contr. run)	64—73	64—73	61—70	1—100	66—75
Years (greenhouse run)	64—73	64—73	61—70	61—80	66—75
Length before int. (AM)	>20 a	>20 a	>20 a	>20 a	>10 a
Length before int. (OM)	>10 000 a	>10 000 a	>400 a	>8 000 a	>200 a
Length of experiment	100 a	100 a	60 a	100 a	75 a
Global warming (C)	1.6	1.3	2.3	2.3	1.7
Global warming MOM	2.6	2.6	4.5	4.0	2.7

Note: Length before int. (AGCM): time length before integration (AGCM). Length before int. (OGCM): time length before integration (OGCM). Length of experiment: length before integration (AGCM). Global warming: global warming at the time CO_2 doubling, AGCM coupled with OGCM. Global warming MOM: global warming at the time $2\times CO_2$, AGCM coupled with mixed layer ocean model. CO_2 concentr. (contr. run): CO_2 concentration in control run. Years (contr. run): the time slice for which the control run outputs have been calculated. Years (greenhouse run): the time slice for which the greenhouse run outputs have been calculated.

The purpose of this paper is to describe the available simulation results in East Asia region

(70°E — 140°E, 15°N — 60°N). The two aspects of the IPCC regional model project are covered: one is the regional climate change induced by increasing CO_2, the other is the regional evaluation of CGCM simulations. In Section II, the CGCM outputs and the observed climate data (1961—1990) are described briefly, and the basic statistical methods are introduced also. Regional climate change induced by increasing CO_2 simulated by these five CGCMs is discussed in Section III. Section IV is the regional evaluation results of these five CGCM simulations. In Section V, a brief summary and main conclusions are given.

II. DATA AND METHOD

In this paper, all analyses have been limited to the East Asia region, encompassing most part of China and its surrounding territories, extending from 15°N to 60°N, 70°E to 140°E. The variables used in the regional climate change analysis and the regional evaluation study include seasonal surface temperature (ST), surface air temperature (SAT), mean sea-level pressure (MSLP), height of 500 hPa (H500), precipitation and soil moisture (SM). In the evaluation section, because the observed ST and SM are not available, only the SAT, MSLP, H500, and precipitation fields are discussed. Unfortunately, for some variable results there were no CGCM outputs in some models, as shown in Table 2. The CGCM outputs are grided at standard T21 grid intervals, although some models are spectral and the others are grid models. The observed grid data have a grid of 10°×10° (for MSLP and H500) and 1°×1° (for SAT and precipitation); therefore, in order to undertake fundamental statistical analysis and plot more conveniently, the CGCM outputs and observed data have been interpolated at a consistent spatial resolution of 5°×5°.

Table 2. Summary of CGCM Outputs

	OPYC	LSG	NCAR	GFDL	HADL
Surface temperature	YYYY	YYYY	YYYY	YNYN	YNYN
Surface air temperature	YYYY	YYYY	YYYY	YNYN	
Mean sea-level pressure	YYYY	YYYY	YYYY		
Height of 500 hPa	YYYY	YYYY			YNYN
Precipitation	YYYY		YYYY		
Soil moisture	YYYY	YYYY	YYYY	YNYN	YNYN
Interannual variance	YYYY				

Note: YYYY: available in four seasons; YNYN: available in summer and winter; BLANK: without output, *Interannual variance*: only available for ST, MSLP and H500.

The definition of the region is mainly based on the climate background, rather than on the political boundaries. In contrast to other regional studies on climate change and model evaluation, the study focused on East Asia and China is also important and has some special significance. Because, firstly, East Asia region is a very sensitive region to climate and weather impacts in the world, and experiences the most intense monsoon climate in the world. Secondly, since the present global CGCMs are less successful on the regional scale in spite of

the fact that these models succeed on the large scale (Houghton et al. 1990; 1992), the regional evaluation of climate simulations is more helpful for modellers to develop the model and more important to confirm the significant levels of future climate change scenarioes produced by CGCMs.

In the evaluation section (Section IV), the similarity of simulated and observed fields is primarily measured with the following fundamental statistical quantities:

Mean (μ) series: measures the difference of means, μ: regional mean, $\mu_m - \mu_o$: regional difference between the simulated and observed, $(\mu_m - \mu_o)/\sigma$: relative errors measured with standard deviation σ. Variance (σ) series: measures the difference of variance, σ: standard deviation (for spatial fields), S_m/S_o: ratio of variance (for spatial fields) between simulated and observed. Correlation coefficient (γ): measures the similarity of spatial distribution, γ: correlation coefficient between simulated and observed spatial fields. Root-mean-square error (RMSE) series: measures absolute errors and systematic errors, $RMSE1$: root-mean-square error, $RMSE2$: root-mean-square error, but with the systematic error removed. For the two equivalent fields, $\mu_m - \mu_o$ and $(\mu_m - \mu_o)/\sigma = 0$, $S_m = \sigma^2$, $S_m/S_o = 1$, $\gamma = 1$, $RMSE1 = 0$ and $RMSE2 = 0$.

III. REGIONAL CLIMATE CHANGE INDUCED BY INCREASING CO_2

The transient response of the climate system to increasing greenhouse gases can be simulated reliably only with a global coupled atmosphere and ocean general circulation model (Houghton et al. 1990; 1992). Because of the limit of the computer resources, in fact, there have been only a few such simulations — NCAR, GFDL, DKRZ OPYC, DKRZ LSG, UKMO. Since different CGCMs have different vertical and horizontal resolutions, different sub-grid process parameterizations, different flux correction schemes (in order to remove the climate drift), even different models employ different greenhouse gas forcing schemes, ranging from a linear increase of 1%/a to the nonlinear increase such as scenarioes A and D of IPCC (Washington and Meehl 1989; Stouffer et al. 1989; Murphy 1992; Cubasch et al. 1992; 1994; Cess et al. 1991), of course, there are some differences of transient response between models. In fact, simulated climate changes by these models share a lot of common characteristics in many aspects .

1. *Regional Average Climate Change*

The simplest climate change scenario is the model average of $2 \times CO_2$ minus $1 \times CO_2$. Table 3 summarizes the results of the regional average climate change simulated by these CGCMs. From that it can be found that, for CO_2 doubling, the sensitivities of annual mean SAT and ST range from 1.37℃ to 2.6℃ and from 1.3℃ to 3.1℃ respectively and the composite values (model averaged) are 1.94℃ and 2.13℃ respectively. Taking the four seasons into account, the warming in winter is the largest, the model averaged warming is 2.26℃ and 2.42℃ for SAT and ST respectively, but that in summer is the smallest, the corresponding values are only 1.57℃ and 1.6℃. The warming in spring and autumn is between those in winter and summer. These are true for the individual model, but there is obvious difference in warming amplitude between models. In particular, the SAT and ST increases simulated by GFDL and HADL are remarkably higher than those produced by other

models. In contrast, there is lowest warming in NCAR model. It is noticeable that the regional average warming amplitudes in most models are larger than those of the global average except for NCAR model.

In all models, regional average MSLP decreases and H500 increases both in winter and summer. The regional average increases of seasonal H500 are of the order of 30—50 m in most models. However, the H500 increase in HADL model is much bigger than that in OPYC and LSG models. In addition, the difference of H500 increase from season to season is very small in OPYC model, but large in LSG model, and its winter increase is over 10 m larger than that in summer. For the seasonal MSLP, these experiments indicate a slight decrease in the regional average in four seasons except NCAR summer result . The model averaged decrease is

Table 3. Simulated Seasonal Changes in the Regional Average

	OPYC	LSG	NCAR	GFDL	HADL	Comp.
			Surface atmosphere temperature (℃)			
Spring	1.9708	1.5624	1.6782			1.7371
Summer	1.7556	1.2059	0.9034	2.3901		1.5638
Autumn	2.1331	1.6686	1.4960			1.7659
Winter	2.3214	2.5061	1.4195	2.8064		2.2634
Annual	2.0452	1.7358	1.3743	2.5983		1.9384
			Surface temperature (℃)			
Spring	1.9376	1.5424	1.6521			1.7107
Summer	1.7390	1.1933	0.7431	2.3584	2.9150	1.7898
Autumn	2.1237	1.6467	1.4844			1.7516
Winter	2.2753	2.4780	1.3136	2.7463	3.2633	2.4153
Annual	2.0189	1.7151	1.2983	2.5523	3.0891	2.1348
			Mean sea-level pressure (hPa)			
Spring	−0.5705	−0.1589	−0.9521			−0.5605
Summer	0.0166	0.2556	−0.6308			−0.1195
Autumn	−0.3729	−0.0150	−0.4871			−0.2917
Winter	−0.8036	−0.2836	−0.6614			−0.5829
Annual	−0.4326	−0.0505	−0.6829			−0.3886
			Height of 500 hPa (m)			
Spring	36.7736	32.3300				34.5518
Summer	39.7250	29.5071			50.1043	39.7788
Autumn	39.3193	34.3936				36.8564
Winter	34.9086	41.2579			54.3271	43.4979
Annual	37.6816	34.3722			52.2157	41.4232
			Precipitation (%)			
Spring	20.5392		12.3034			16.4213
Summer	10.4978		13.1438			11.8208
Autumn	6.8344		6.8764			6.8554
Winter	6.9779		4.8317			5.9048
Annual	11.2123		9.2888			10.2506
			Soil moisture (cm)			
Spring	0.3281	0.2943	0.1001			0.2408
Summer	0.0861	−0.0803	0.1658	−0.3103	−0.2213	−0.0720
Autumn	0.2134	−0.0132	0.0013			0.0672
Winter	0.2428	0.1892	0.0494	−0.1091	−1.2085	−0.1672
Annual	0.2176	0.0975	0.0791	−0.2097	−0.7149	−0.1061

Note: Comp. : Model averaged value.

more obvious in spring and winter than that in summer and autumn, and it is also true for most individual models.

The model average of the regional average precipitation change shows a slight increase in autumn and winter, but a significant increase in summer and spring, about 10%. As a large part of the total year precipitations is owing to the summer precipitation in East Asia, the absolute increase of summer precipitation is much larger than that in the other seasons. Additionally, the amplitudes of precipitation change in OPYC and NCAR are very similar to each other. Unlike the other variables, SM changes are more complex. It is very general that there are substantial differences in most seasons from model to model. However, SM increases in spring are produced by all experiments available. SM increases in all seasons in OPYC and NCAR results, but decreases in summer and winter in GFDL and HADL results, increases in spring and winter and decreases in summer and autumn in LSG results. The maximum SM decrease is found in HADL winter results, with a value of 1.21 cm.

2. *Regional Distribution of Climate Change*

From the difference fields of seasonal and annual mean ST between simulated and observed (not shown), it can be seen that for all seasons and annual mean the warming is very obvious in most areas. One main feature, most clearly shown by the composite fields, is that the simulated warming is generally stronger in winter than in summer, more evident in higher latitudes than in lower latitudes, and the warming in land areas is stronger than in ocean areas. The annual mean warming is between 1.5℃—3.0℃ in most areas, which is larger than the global mean. There is a satisfactory consistency in the simulated warming in all seasons between models, especially in the simulated warming in middle-low latitudes. Generally, the warming differences from model to model are about 0.5℃ or much less; the maximum differences between models occur near the Japan Island, with the values being up to 3℃. The features of SAT changes are very similar to those of ST, but with a slight smaller amplitude. For the summer cases, the warming in composite field ranges from 1.25℃ to 2.5℃.

The winter composite MSLP fields indicate a slight increase in the area south of 40°N and west of 100°E, generally smaller than 1 hPa, and a decrease in the remaining large area. In general, the decrease in middle-high latitudes is larger than that in middle-low latitudes and larger in the west than in the east as shown in Fig. 1 and Fig. 2. The maximum decrease (1.5 hPa) is found in the area extending from 40°N to 55°N and from 120°E to 170°E. The other feature in winter MSLP change pattern is that most models show an obvious east-west isotimic distribution in the eastern part of East Asia, but north-south distribution in the west areas. And there are larger spatial differences of MSLP change in NCAR model than in others, for example, the maximum decrease in NCAR model is as high as 3 hPa, and the maximum increase is about 2 hPa. In contrast, the spatial differences in LSG model are relatively small. As a whole, there is a satisfactory consistency of MSLP change pattern in winter from model to model. In summer results, most areas except the areas south of 45°N and west of 110°E show decreases of MSLP, and the amplitude of the MSLP change is much smaller in winter. For the composite fields, the most evident decrease is found around the Korea Peninsula, the value is only about 0.5 hPa, and there are several scattering small increase centers of 0.5 hPa. This pattern corresponds the slight weakness of the center of Indian low and the expanding

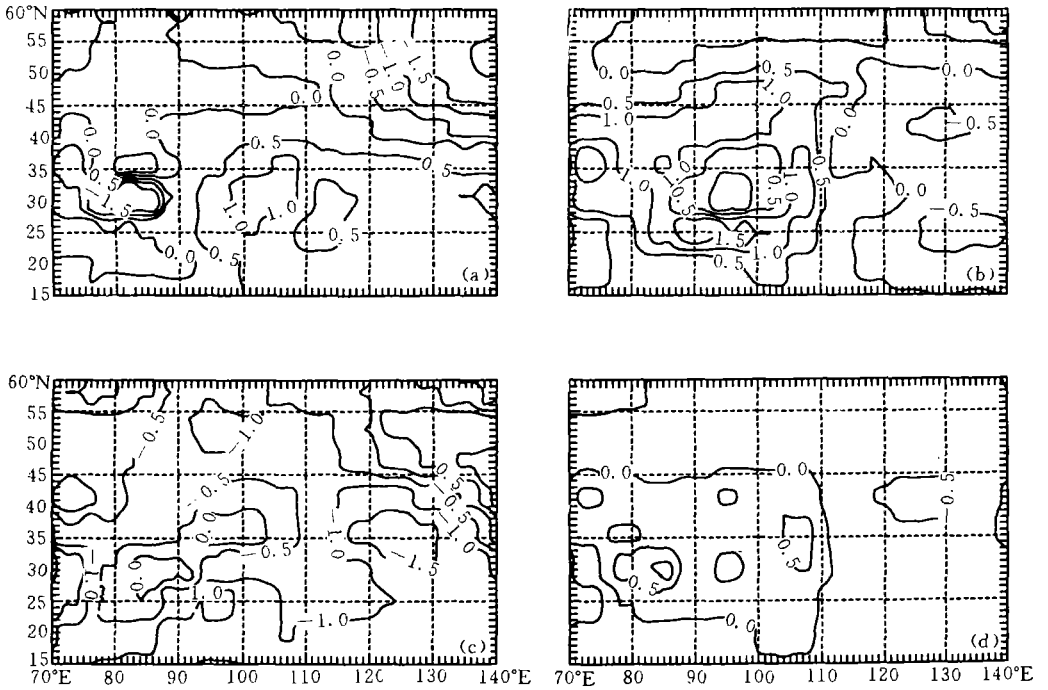

Fig. 1. The simulated changes in mean sea-level pressure in summer. (a) OPYC: (b) LSG: (c) NCAR: (d) average of (a) — (c).

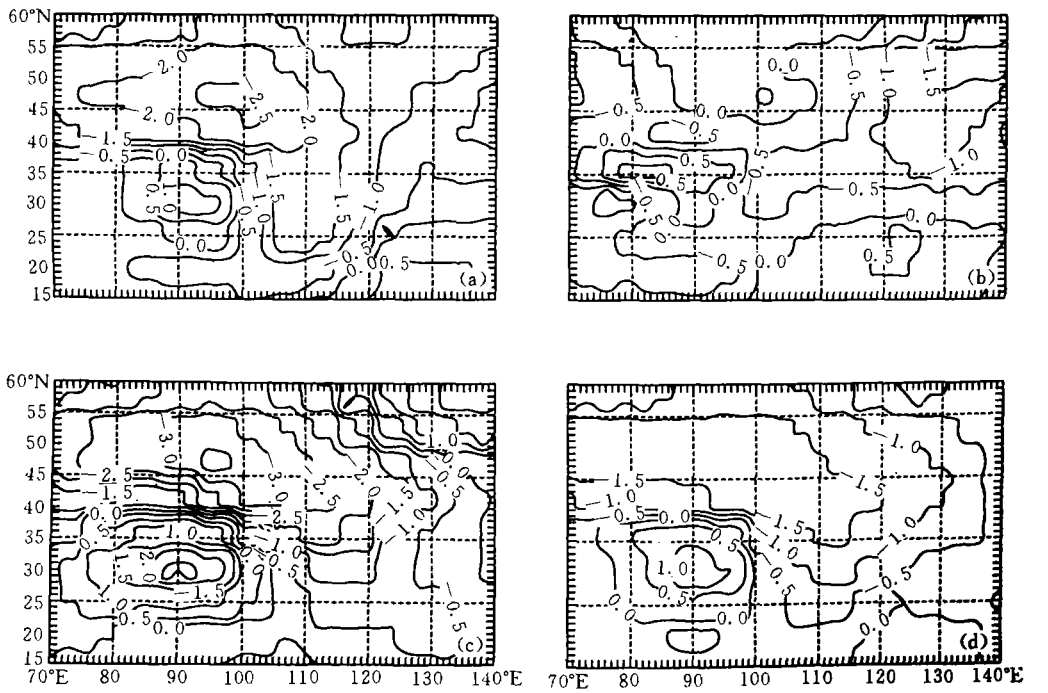

Fig. 2. As in Fig. 1, but for winter.

towards north and east of Indian low, i. e., the strengthening of the summer monsoon in East Asia. In comparison with the winter cases, there is large difference in the MSLP change pattern from model to model in summer, even in some areas here are different biases between OPYC and NCAR model.

The winter H500 simulated by all models increases in the whole area. The amplitude increase in HADL model is the biggest, with the maximum value in HADL results exceeding 80 m, occurs in the central and eastern areas near 45°N. In HADL and LSG models, the H500 increase in middle-low latitudes is lower than that in middle-high latitudes, but it is adverse in OPYC model. The main feature of H500 change pattern in the composite fields is similar to that in HADL simulation, but with a smaller amplitude. This pattern corresponds the weakness of East Asia trough in winter, and the smaller north-south gradient of H500. The change pattern of the summer H500 fields is similar to that in winter. For the composite fields, the increase is large in middle-low latitude areas than in middle-high latitude areas and this is also true for OPYC and LSG results. This pattern corresponds the strengthening and expanding towards west of subtropical high in summer and the bigger north-south gradient of H500 fields. It is interesting that, unlike the winter cases, the increase in OPYC is larger than that in LSG, and the pattern in HADL is adverse to that in OPYC and LSG.

Considering the obvious monsoon climate in East Asia, summer precipitation is mainly focused on, as shown in Fig. 3. For the composite results, the precipitation increases over 10% in most areas, and decreases under 10% in some local areas west of 120°E and near 40°N. Two remarkable regions with relatively large summer precipitation increase are the Indian continent (about 50%) and Northeast China (about 30%). It is noticeable that the precipitation increase exceeds 10% in most monsoon areas (i. e., the south and east part of

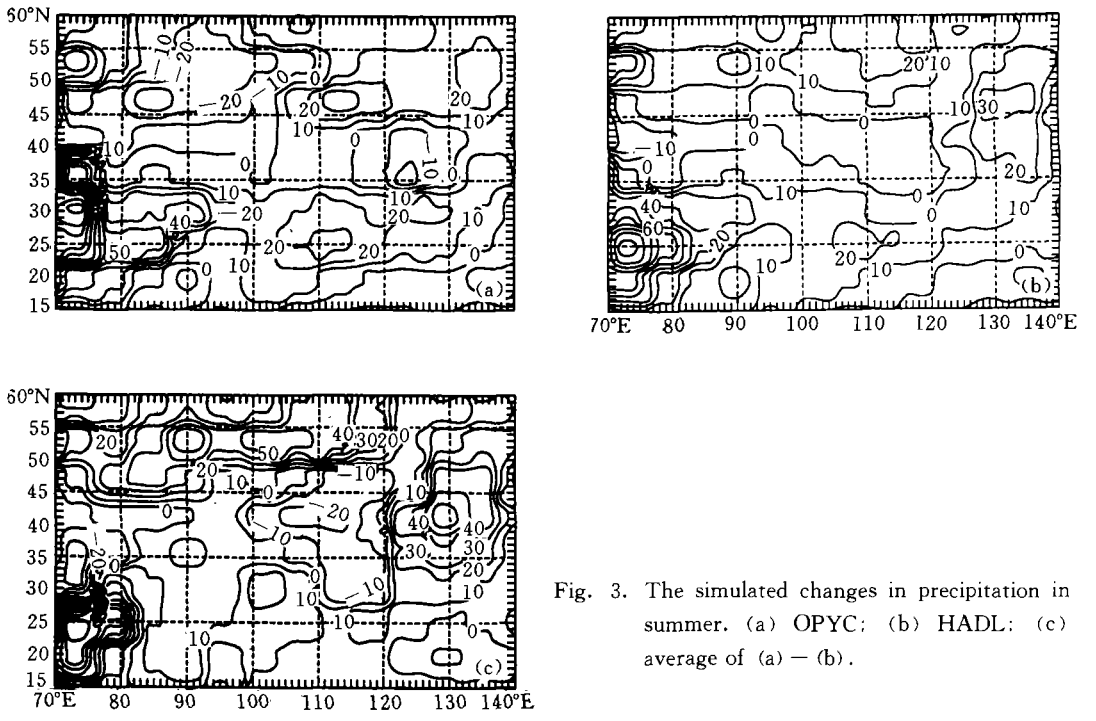

Fig. 3. The simulated changes in precipitation in summer. (a) OPYC; (b) HADL; (c) average of (a) — (b).

China) except the Huanghe River basin with a slightly decrease. For the annual precipitation, the main features are similar to those in summer. In contrast to the other variables, the differences of the precipitation change fields between different models are very large. Especially, for the summer precipitation in the areas with latitudes between 35°N — 45°N, there are different change biases between OPYC and NCAR models, and the differences between models are rather small in the areas south of 35°N and ocean areas.

SM changes are more complex than the other variables. There is a little consistency between models in SM change patterns. For the composite spring fields, there is an evident SM increase area located near 40°N in the west part of East Asia, the increase value exceeding 1 cm. The SM increases in most areas north of 30°N and decreases in the west areas south of 35°N. But for summer cases, the SM change pattern is exactly adverse to that in spring, SM increasing in the south areas and decreasing in the north areas. As mentioned above, there are little consistencies of SM change fields from model to model whether in spring or in summer, but the differences between models in low latitudes are relatively small; especially for the summer cases, all experiments indicate increase in these areas. Additionally, the sensitive areas of SM change in autumn are mainly located north of 35°N, but in winter are located south of 35°N. Since there are different SM change biases in different seasons, the annual SM changes are smaller than those in the individual seasons.

IV. EVALUATION OF CGCM REGIONAL SIMULATION

Observed data fields used here are seasonal SAT, MSLP, H500 and precipitation for the comparison of seasonal means between simulated and observed. For the comparison of interannual variance fields, because SAT fields are not available for the MPI CGCM, ST is used instead of SAT. Because ST fields from the CGCM have been averaged over all weather conditions and time of day, there should be a little difference between SAT and ST fields. In the comparison of spatial distributions between simulated and observed, the differences of large scale patterns are emphasized, rather than the local details. Some test statistics are employed to estimate the difference between two spatial fields as mentioned in Section II.

1. *Seasonal Mean Surface Atmosphere Temperature*

The SAT fields simulated by most CGCMs over East Asia are systematically lower than the observed, in the four seasons and annual means. The systematic error is of the order of about 5℃. The main features of geographic distributions of errors exhibit higher in the west and lower in the east of East Asia. For example, for the model averaged SAT fields, in the area east of the 100°E, the errors are often smaller than 5℃, and vice versa. Particularly in the annual mean and summer figures (not shown), NCAR model is the best one of these 4 CGCMs in simulating SAT fields. For the annual mean SAT, the systematic errors are generally lower than 2.5℃; especially in the east part of China in summer, the errors are very low. In winter these values are slightly large, about 3℃ — 5℃. The GFDL simulation takes the second place to reproduce the SAT fields, especially in the structure of SAT geographic distribution. But its winter errors are too large, about 10 ℃. From Table 4 it can be also found that NCAR and GFDL reproduce seasonal and annual mean SAT with greater accuracy than others . Especially , NCAR gives the most satisfactory results in RMSEs and regional

Table 4. Statistical Comparison between Simulated and Observed Surface Atmosphere Temperatures (K)

Summer								
	μ	$\mu_m-\mu_o$	$(\mu_m-\mu_o)/\sigma$	σ	S_m/S_o	γ	*RMSE*1	*RMSE*2
OPYC	287.645	−6.857	−1.374	6.554	1.724	0.512	9.023	5.864
LSG	287.454	−7.048	−1.412	8.152	2.667	0.504	10.003	7.099
NCAR	293.857	−0.645	−0.129	4.258	0.728	0.457	4.902	4.859
GFDL	288.905	−5.597	−1.121	5.915	1.404	0.664	7.212	4.548
Comp.	289.465	−5.037	−1.009	5.783	1.342	0.576	7.103	5.007
Obs.	294.502	0.000	0.000	4.992	1.000	1.000	0.000	0.000
Winter								
	μ	$\mu_m-\mu_o$	$(\mu_m-\mu_o)/\sigma$	σ	S_m/S_o	γ	*RMSE*1	*RMSE*2
OPYC	262.743	−6.078	−0.651	10.922	1.369	0.941	7.181	3.825
LSG	260.249	−8.573	−0.918	11.953	1.639	0.856	10.609	6.249
NCAR	265.016	−3.805	−0.408	9.679	1.075	0.949	4.883	3.060
GFDL	257.268	−11.553	−1.238	8.511	0.831	0.903	12.233	04.02
Comp.	261.319	−7.503	−0.804	9.902	1.125	0.943	8.189	3.283
Obs.	268.822	0.000	0.000	9.335	1.000	1.000	0.000	0.000
Annual								
	μ	$\mu_m-\mu_o$	$(\mu_m-\mu_o)/\sigma$	σ	S_m/S_o	γ	*RMSE*1	*RMSE*2
OPYC	275.802	−6.649	−1.070	8.482	1.863	0.804	8.368	5.082
LSG	274.706	−7.745	−1.246	9.679	2.426	0.680	10.510	7.105
NCAR	280.400	−2.050	−0.330	5.376	0.748	0.833	4.012	3.448
GFDL	273.086	−9.364	−1.507	5.934	0.912	0.851	9.936	3.321
Comp.	275.999	−6.452	−1.038	7.072	1.295			
Obs.	282.45	0.000	0.000	6.215	1.000	1.000	0.000	0.000

Note: (1) Comp. —model averaged; Obs. —observed fields. (2) μ: regional mean; $\mu_m-\mu_o$: simulated minus observed; $(\mu_m-\mu_o)/\sigma$: ratio between $(\mu_m-\mu_o)$ and σ; σ: standard deviation; S_m/S_o: variance ratio between simulated and observed; γ: correlation coefficient; *RMSE*1: root-mean square error; *RMSE*2: root-mean square error, but systematic error removed. Same meanings in the following tables.

means for each season and annual mean SAT fields, in correlation coefficient and variance for the winter season. GFDL performs best in γ both in summer and annual mean. Considering the calculated RMSEs and μ, it is easily concluded that the systematic errors in NCAR model are smallest, with the smallest difference in regional mean and almost the same values of *RMSE*1 and *RMSE*2. Apart from the NCAR run, there is a clear systematic tendency in the

simulated SAT field, and all the remaining models exhibit a significant cold bias in both seasonal and annual means. It is worth noting that GFDL model produces the largest cold bias, but performs the most satisfactory simulations in γ. As indicated by σ, μ, and γ, most models give the better results in winter than in summer. Although most models produce large systematic errors in simulating seasonal SAT fields, the principle features of seasonal and annual mean SAT fields are correctly reproduced. However, LSG simulation gives far less realistic results in winter than in summer. The spatial distribution of the ratio field between the error and the standard deviation (of interannual variance) is very similar to that of the error field.

2. *Seasonal Mean Sea-Level Pressure*

All three CGCMs, OPYC, NCAR, LSG, successfully reproduce the seasonal mean MSLP fields as shown in Table 5. Especially there are no obvious systematic errors in OPYCresults. The differences between the simulated and observed are lower than 2.5 hPa in most areas both in summer and winter. The maximum differences are found in the small area centered on 30°N and 95°E. The OPYC model unambiguously gives the best results in four seasons. An inspection of RMSE and σ shows that OPYC model has the least difference as compared to observed. When the systematic errors are subtracted, the resulting RMSEs are only about 1.7 hPa both in summer and winter. NCAR gives very similar results as OPYC does in winter, but in NCAR summer results there are big systematic errors. Particularly, the errors in most areas north of the 30°N are larger than 10 hPa. NCAR performs best in the spatial pattern of winter MSLP, with the highest γ of 0.87, but fails to reproduce σ. For

Table 5. Statistical Comparison between Simulated and Observed Mean Sea-Level Pressures (hPa)

Summer								
	μ	$\mu_m-\mu_o$	$(\mu_m-\mu_o)/\sigma$	σ	S_m/S_o	γ	*RMSE*1	*RMSE*2
OPYC	1004.125	−0.510	−0.296	4.361	6.429	0.700	1.725	1.706
LSG	1000.346	−4.289	−2.494	6.810	15.675	0.820	3.506	2.762
NCAR	993.396	−11.239	−6.534	8.615	25.083	0.657	6.828	3.823
Comp.	999.289	−5.346	−3.108	5.971	12.051	0.798	3.587	2.372
Obs.	1004.635	0.000	0.000	1.720	1.000	1.000	0.000	0.000
Winter								
	μ	$\mu_m-\mu_o$	$(\mu_m-\mu_o)/\sigma$	σ	S_m/S_o	γ	*RMSE*1	*RMSE*2
OPYC	1025.739	−1.492	−0.299	6.699	1.798	0.855	1.937	1.785
LSG	1024.298	−2.933	−0.587	7.396	2.192	0.759	2.854	2.443
NCAR	1027.178	−0.053	−0.011	2.697	0.291	0.867	1.499	1.498
Comp.	1025.738	−1.493	−0.299	5.374	1.157	0.849	1.630	1.446
Obs.	1027.231	0.000	0.000	4.996	1.000	1.000	0.000	0.000

summer case, σ is too large, and for the winter case, σ is too small. However, LSG produces relatively poor results in μ, γ, σ and RSME, especially in winter fields. Additionally, the error isolines in NCAR figure (not shown) extend latitudinally, but those in LSG extend longitudinally. Considering the interannual variance, it is concluded that simulated MSLP errors are smaller than SAT errors in all models. As the SAT fields exhibit, regardless of the measurement used, the simulated winter MSLP fields are more realistic than the summer fields. This is most evident in NCAR simulations.

3. *Seasonal Mean 500 hPa Height*

Most CGCMs succeed in simulating the main characteristics of the spatial distribution of H500 fields, but in general, the H500 fields simulated by these CGCMs are systematically lower than the observed. The typical errors range from 30 m to 50 m. Taking the interannual variance of the H500 seasonal mean fields into account, the systematic errors are smaller than those of SAT and MSLP. HADL succeeds best to reproduce H500 fields as well in winter as in summer, as shown in Fig. 4 and as indicated by high γ and other statistics in Table 6. The errors in most areas south of 45°N are about 20 m lower than the observed, but slightly bigger in the area north of 45°N. Because the interannual variance in middle-high latitudes is several times larger than that in middle-low latitudes, the errors in the north areas are not very large. OPYC produces slightly poorer results than HADL does, and the summer H500 fields in OPYC results exhibit about 20 — 40 m lower than the observed in most areas, but for the winter fields the differences between the simulated and observed are larger than 40 m in most areas. In LSG simulations, the results are in most respects similar to those in OPYC.

Table 6. Statistical Comparison between Simulated and Observed Heights of 500 hPa (m)

Summer								
	μ	$\mu_m-\mu_o$	$(\mu_m-\mu_o)/\sigma$	σ	S_m/S_o	γ	*RMSE*1	*RMSE*2
OPYC	5777.313	−35.370	−0.690	58.220	1.289	0.936	20.633	10.430
LSG	5798.726	−13.957	−0.272	24.557	0.229	0.878	17.556	16.089
HADL	5785.958	−26.725	−0.521	53.526	1.089	0.979	14.552	5.553
Comp.	5787.333	−25.351	−0.494	44.466	0.752	0.963	14.745	7.391
Obs.	5812.683	0.000	0.000	51.289	1.000	1.000	0.000	0.000
Winter								
	μ	$\mu_m-\mu_o$	$(\mu_m-\mu_o)/\sigma$	σ	S_m/S_o	γ	*RMSE*1	*RMSE*2
OPYC	5537.241	−45.717	−0.296	166.953	1.167	0.987	27.258	14.613
LSG	5547.245	−35.713	−0.231	145.464	0.886	0.993	20.692	10.250
HADL	5526.517	−56.441	−0.365	178.514	1.334	0.998	31.344	13.244
Comp.	5537.001	−45.958	−0.297	163.188	1.115	0.995	24.788	8.910
Obs.	5582.958	0.000	0.000	154.532	1.000	1.000	0.000	0.000

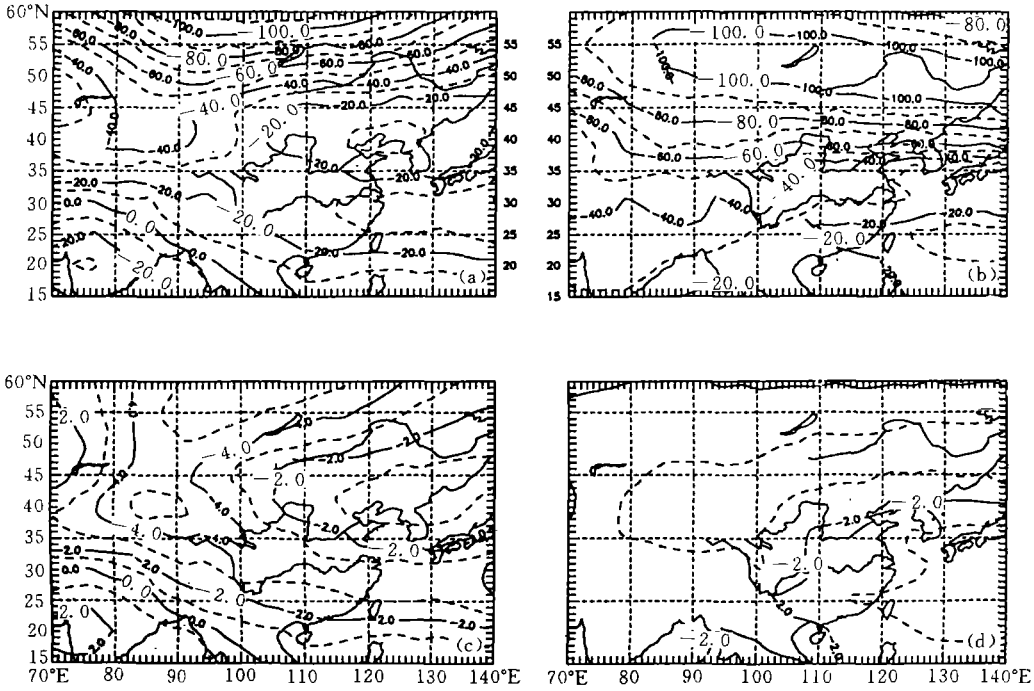

Fig. 4. H500 error (simulated minus observed) and ratio (of error to standard deviation) fields as given by HADL error fields: (a) summer; (b) winter. ratio fields; (c) summer; (d) winter.

however, with slightly bigger errors. Although LSG presents the least RMSEs and μ difference, it reproduces relatively poor values in S_m/S_o, too small in summer and too large in winter. In comparison with SAT and MSLP, H500 fields are more successfully reproduced by most models.

4. *Seasonal Mean Precipitation*

The IPCC data set contains precipitation data for only two models: OPYC and NCAR. In contrast to the simulated SAT, MSLP and H500 fields, the precipitation fields are simulated with the least accuracy by the two models available (Table 7). There are noticeable differences between the simulations and the observations as well in four seasons as in annual means. The annual mean precipitation is generally overestimated in most areas. The typical errors are of the order of 2 mm/d. The summer results are similar to annual means. The ratios of the absolute errors to the standard deviation are larger than 10 in most areas except the areas with large summer precipitation: East China and Southwest China. However, OPYC is better than NCAR model in modeling precipitation. It gives a relatively small RMSE and μ difference, a little larger value of S_m/S_o. As indicated by low γ, NCAR produces far less satisfactory results, its summer γ is only 0.27, and its S_m is about 5 times larger than the observed. Like the simulated SAT, MSLP and H500 fields, the simulated precipitation fields are relatively better in winter than in summer. In OPYC simulations, the ratios between the errors and standard deviations are relatively large in the above mentioned high error areas, but relatively small in the Changjiang River basin and South China. Although the errors in winter are

smaller than those in summer. typical error is about 1 mm/d. but because there is little precipitation in most areas except the low-latitudes areas. the ratios between the errors and standard deviations are much larger than those in summer.

5. *Interannual Variance*

OPYC model is the only one with the outputs of interannual variance of seasonal means. As shown by Fig . 5 . the simulated SAT interannual variances are larger than the observed both in summer and in winter. For example. the ratios between the simulations and the observations of summer SAT interannual variance are larger than 2 in most areas except the small area between Changjiang River and observed interannual variances are much bigger than those in summer. and the ratio is larger than 4 in most areas. But for the winter SAT. the results are slightly better. and especially in the Northeast. the West and the Southeast of China. the ratios are close to 1. However. the ratios in the areas between Changjiang River and Huanghe River are usually larger than 1. For the MSLP interannual variance fields. the simulation results are more realistic than SAT simulation. and the ratios are about 0. 5 in most areas in summer. about 1 in most areas in winter except the area close to Qinghai-Xizang Plateau. In contrast to the SAT and MSLP interannual variance fields. the interannual

Table 7. Statistical Comparison between Simulated and Observed Precipitations (mm/d)

Summer								
	μ	$\mu_m-\mu_o$	$(\mu_m-\mu_o)/\sigma$	σ	S_m/S_o	γ	*RMSE*1	*RMSE*2
OPYC	4. 446	1. 434	0. 645	3. 042	1. 874	0. 648	2. 736	2. 330
NCAR	5. 843	2. 830	1. 274	4. 882	4. 829	0. 274	5. 554	4. 779
Comp.	5. 145	2. 132	0. 960	3. 257	2. 148	0. 508	3. 569	2. 862
Obs.	3. 013	0. 000	0. 000	2. 222	1. 000	1. 000	0. 000	0. 000
Winter								
	μ	$\mu_m-\mu_o$	$(\mu_m-\mu_o)/\sigma$	σ	S_m/S_o	γ	*RMSE*1	*RMSE*2
OPYC	1. 200	0. 851	1. 472	0. 915	2. 510	0. 759	1. 045	0. 607
NCAR	2. 027	1. 678	2. 904	1. 224	4. 487	0. 737	1. 898	0. 888
Comp.	1. 614	1. 264	2. 188	0. 954	2. 729	0. 837	1. 386	0. 567
Obs.	0. 349	0. 000	0. 000	0. 578	1. 000	1. 000	0. 000	0. 000
Annual								
	μ	$\mu_m-\mu_o$	$(\mu_m-\mu_o)/\sigma$	σ	S_m/S_o	γ	*RMSE*1	*RMSE*2
OPYC	2. 800	1. 314	0. 969	1. 707	1. 586	0. 697	1. 803	1. 235
NCAR	3. 632	2. 147	1. 584	1. 931	2. 029	0. 471	2. 776	1. 760
Comp.	3. 216	1. 730	1. 277	1. 513	1. 246	0. 694	2. 067	1. 131
Obs.	1. 486	0. 000	0. 000	1. 355	1. 000	I. 000	0. 000	0. 000

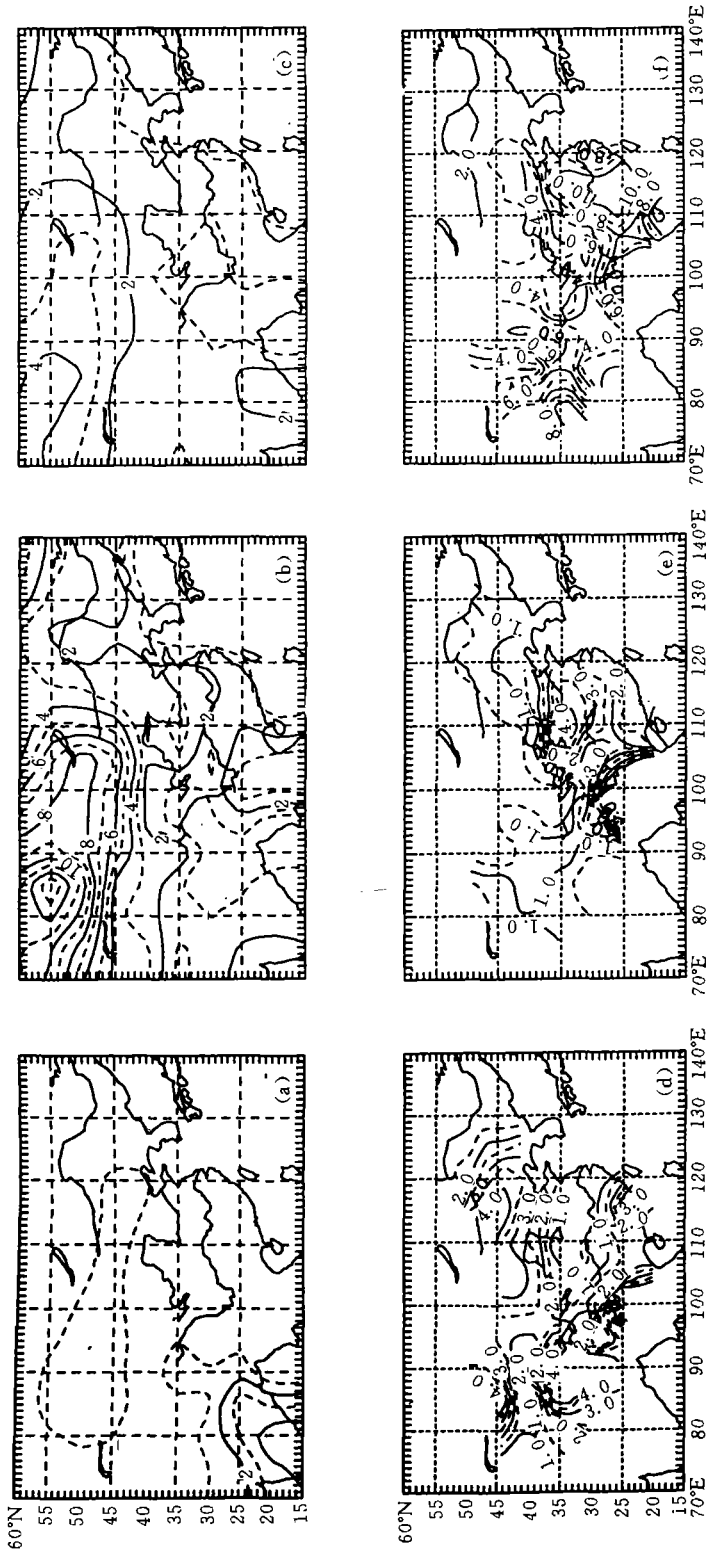

Fig. 5. Interannual variance fields as given by OPYC and ratio fields between observed and simulated interannual variance of surface air temperature and interannual variance fields: (a) summer; (b) winter; (c) annual mean. ratio fields: (d) summer; (e) winter; (f) annual mean.

variance fields of simulated precipitation are better in summer, but worse in winter and in annual means. In addition, the simulated precipitation variances in the east monsoon regions of China are relatively realistic, and the ratios are close to 1; but in West China, these values are too big.

V. CONCLUSION

Preliminary results from the latest integration of the global CGCMs with increased CO_2 show that, in spite of the differences in transient response patterns between models, all of the models exhibit a number of similar overall features in their responses. Some features of the regional climate change, when carbon dioxide concentrations are doubled, are produced by most models. The simulated regional averaged increases of annual mean ST and SAT at the time of effective CO_2 doubling range from 1.6℃ to 2.6℃, and 1.3℃ to 3.1℃ respectively, which is larger than the global averaged. The same overall characteristics are seen in the distributions of the ST and SAT change patterns simulated by these models. These characteristics are: (1) The surface warming at high latitudes is greater than that at low latitudes; the surface warming in winter is more significant than that in summer and other seasons; and the surface warming over land areas is larger than that over ocean areas at the same latitude. (2) The regional averaged MSLP decreases, and the H500 increases in all seasons and in all models. The spatial patterns of the simulated MSLP and H500 changes correspond to the strengthening of the summer monsoon circulation in the East Asia region and the weakness of the wind fields in winter. (3) The precipitation increases. In particular, the summer precipitation in the monsoon area increases significantly. Additionally, regional mean annual soil moisture decreases, but there is little consistency between models in spatial distribution.

On the basis of the visual and fundamental statistical comparison between the CGCM control run and the observed climate data, it is concluded that: (1) These five CGCMs are particularly good in simulating spatial distribution of present climate in the East Asia region. In particular, the main characteristics of the seasonal mean H500, SAT, MSLP fields can be simulated by most CGCMs. But there are significant systematic errors in SAT, MSLP, H500 fields in most models. In general, the simulated seasonal mean SAT, MSLP, H500 errors are of the order of 5 ℃, 3—4 hPa, and 30 m, respectively. (2) Taking the four seasons into account, the distribution of SAT was best described in NCAR and GFDL simulations; DKRZ OPYC is the best of these CGCMs in simulating the MSLP and precipitation fields; HADL succeeds best in simulating H500 fields. On the whole, DKRZ OPYC is the best in simulating the present climate in the East Asia region. (3) In most models, H500 fields are best simulated, and SAT and MSLP are the next best. The precipitation fields are simulated with the least accuracy. There are noticeable differences between the models and observed seasonal mean precipitation fields. (4) In most models, simulations of seasonal and annual mean variable fields are most accurate for the winter season and least accurate for the summer season.

Although these two aspects, regional climate change and regional evaluation of climate simulation, have not been combined in this paper, it should be easily concluded that the simulated changes of SAT fields are more reliable than those of precipitation and soil moisture.

It is difficult to rank these 5 CGCMs in reliability, because there are a few variable fields of model outputs for HADL and GFDL. From the limited information, on the whole, DKRZ OPYC succeeds best in simulating the climate in the East Asia region: HADL and GFDL take the second place: NCAR and LSG are worse than OPYC, HADL and GFDL.

We would like to thank M. Hulme, T. Wigley, P. Jones, M. Taylor, U. Cubasch, S. Manabe, G. A. Meehl, W. M. Washington, and J. F. B. Mitchell for their contributions to this study.

REFERENCES

Cess, R. D., et al., (1991). Intercomparison of snow-feedback as produced by 17 general circulation models. *Science*. **253**: 888—892.

Cubasch, U., Hasselmann, K. and Hock, H. et al. (1992). Time-dependent greenhouse warming computations with a coupled ocean-atmosphere model. *Climate Dynamics*. **8**: 55—69.

Houghton, J. T., Jenkins, G. J. and Ephraums, J. J. (Eds.) (1990). *Climate Change — The IPCC Scientific Assessment*. Cambridge University Press, Great Britain. 365pp.

Houghton, J. T., Callander, B. A. and Varney, S. K. (Eds.) (1992). *Climate Change 1992 — The Supplementary Report to the IPCC Scientific Assessment*. Cambridge University Press, Great Britain. 200pp.

IPCC WGI (1994a). *Regional Climate Evaluation Workshop*. 7—11 February 1994. Macquarie University, Australia.

IPCC WGI (1994b). *IPCC Workshop on Article 2 of the United Nations Framework Convention on Climate Change*. 17—21 October 1994. Fortaleza, Brazil.

Manabe, S., Stouffer, R. J. and Spelman, M. J. (1991). Transient responses of a coupled ocean-atmosphere model to gradual changes of atmosphere carbon dioxide. Part 1: Annual mean response. *Journal of Climate*. **4**: 785—818.

Manabe, S., Spelman, M. J. and Stouffer, R. J. (1992). Transient responses of a coupled ocean-atmosphere model to gradual changes of atmosphere carbon dioxide. Part 2: Seasonal response. *Journal of Climate*. **5**: 105—126.

Meehl, G. A. and Washington, W. M. (1993). Low-frequency variability and carbon dioxide transient climate change. Part 1: Time averaged of difference. *Climate Dynamics*. **8**: 117—133.

Mitchell, J. F. B. and Ingram, W. J. (1992). Carbon dioxide and climate: mechanisms of changes in cloud. *Journal of Climate*. **5**: 5—21.

Washington, W. M. and Meehl, G. A. (1989). Climate sensitivity due to increased carbon dioxide: experiments with a coupled atmosphere and ocean general circulation model. *Climate Dynamics*. **4**: 1—38.

Washington, W. M. and Meehl, G. A. (1993). Greenhouse sensitivity experiments with penetrative cumulus convection and tropical cirrus albedo effects. *Climate Dynamics*. **8**: 211—223.